ISOL-like beams of ^{22}Al and ^{26}P at FRIB

ISOLDE Workshop 2023

Erik A. M. Jensen — Aarhus Universitet, DK

Outline

- Briefly: FRIB, beam production and beam cooling
- Detection setup: DSSDs and HPGes
- Physics results on ^{22}Al & ^{26}P: β2p, βα, …

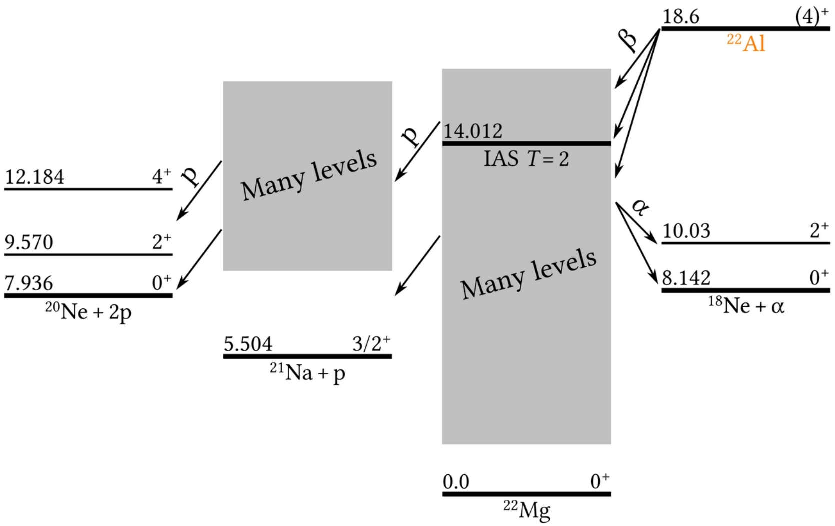

From in-flight beams to ISOL-like beams

- Front End: ^{36}Ar
- Production Target: ^{12}C
- Fragment Separator:
  ~16k pps of ^{22}Al @ 105 MeV/u
- Gas Stopping:
  - 2 helium-filled gas cells – Room Temp. & Cryo
  - Momentum compression and stopping
  - Some filtering of isotopes of interest,
    but also introduction of new contaminants (molecules)
- BECOLA: 5–10 pps of ^{22}Al @ 30 keV
  - Beam of ISOL quality!

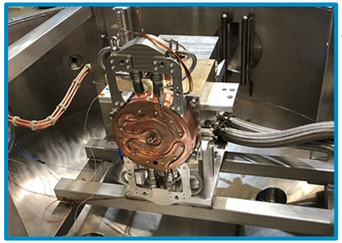

https://frib.msu.edu

Large losses between
Fragment Separator and Gas Stoppers

5–10 pps still an order of magnitude more than previously seen in studies utilising implantation of in-flight beams

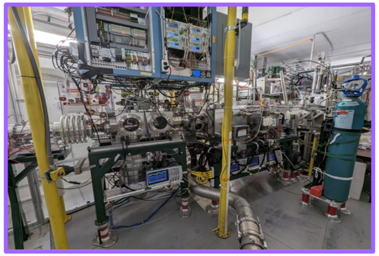

C. Sumithrarachchi

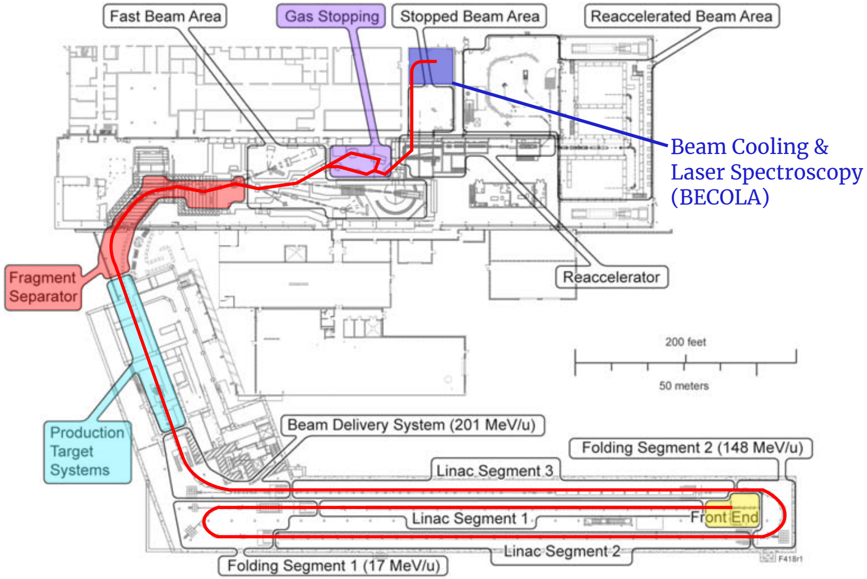

Layout of FRIB.
Adapted from AIP Conf. Proc. **1434**, 94 (2012).

From in-flight beams to ISOL-like beams

- Front End: ^{36}Ar
- Production Target: ^{12}C
- Fragment Separator:
  ~16k pps of ^{22}Al @ 105 MeV/u
- Gas Stopping:
  - 2 helium-filled gas cells – Room Temp. & Cryo
  - Momentum compression and stopping
  - Some filtering of isotopes of interest,
    but also introduction of new contaminants (molecules)
- BECOLA: 5–10 pps of ^{22}Al @ 30 keV
  - Beam of ISOL quality!

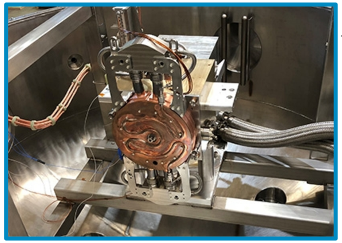

https://frib.msu.edu

Large losses between
Fragment Separator and Gas Stoppers

5–10 pps still an order of magnitude
more than previously seen in studies
utilising implantation of in-flight beams

C. Sumit

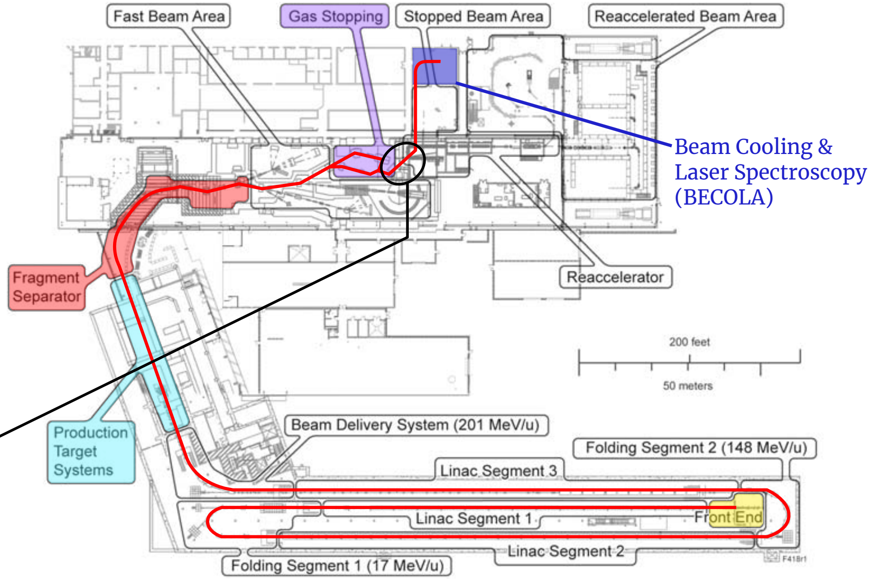

Layout of FRIB.
Adapted from AIP Conf. Proc. **1434**, 94 (2012).

What comes out of the gas cell

- Even with >99 % pure helium gas, various molecules emerge from the gas cell
- Have to pick <u>one</u> mass to send to our detection setup
- For ^{26}P, ^{25}SiH–ligands are also present

	Constrained by cross sections at …	Constrained by chemistry at …
ISOL	Target	Target + Ion Source
In-flight	Target	Gas gell

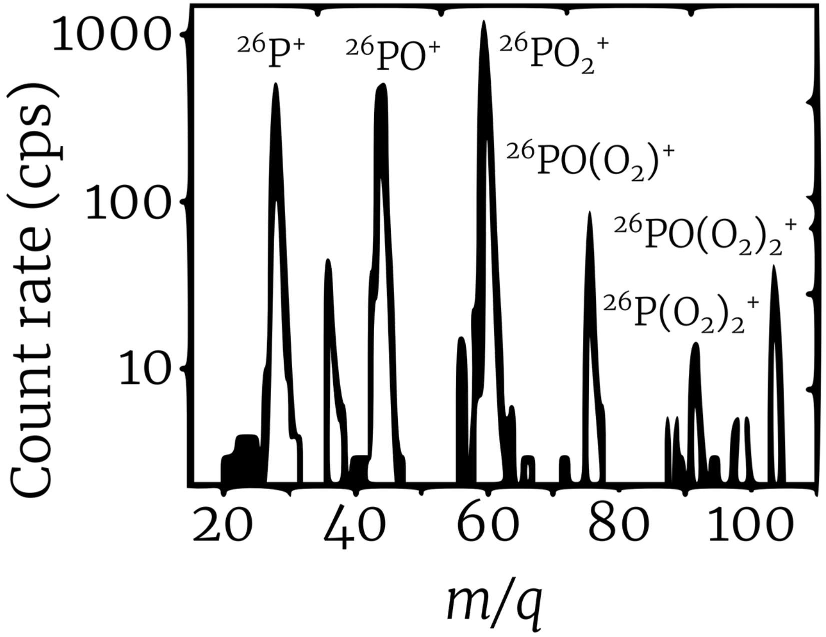

Mass scan just after gas cell.
Courtesy of Chandana Sumithrarachchi, Gas Cell Group at FRIB.

Detection setup

Silicon cube:

- 6 ΔE–E silicon detector telescopes
- ΔE detectors are 16x16 DSSSDs
- ~35 % of 4π for βp/βα

Beam: 30 keV ^{22}Al and ^{26}P stopped in thin carbon foil

Chamber: 2 mm aluminium for low gamma attenuation

Germaniums:

- 2 mechanically cooled coaxial HPGes
- Overall efficiency at 1 MeV ~2 %

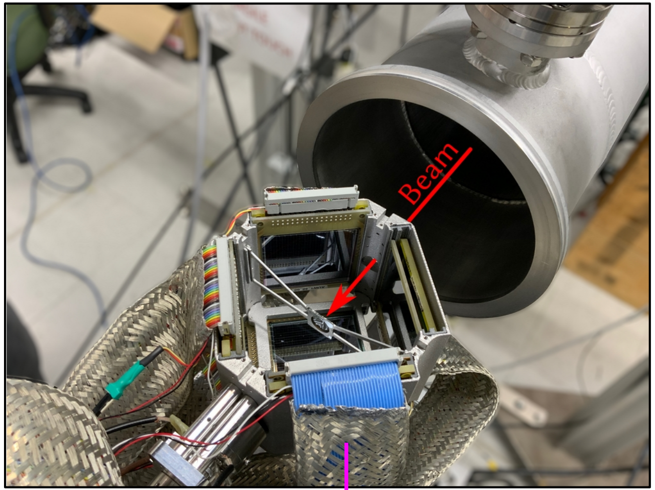

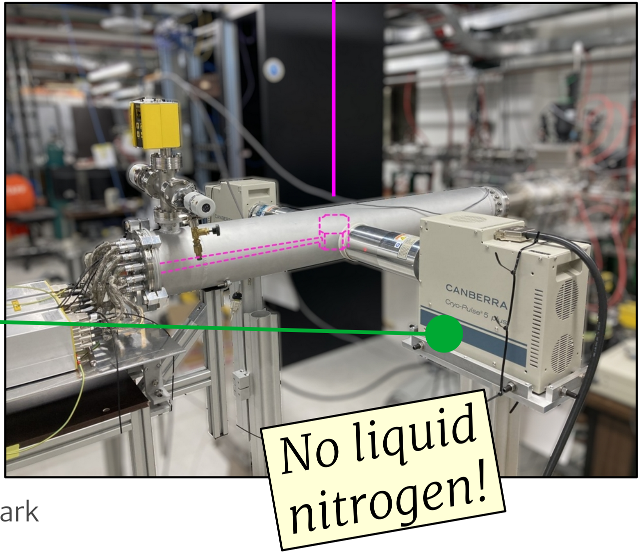

Silicon cube

- 6 ΔE-E silicon detector telescopes
- ΔE detectors are 16x16 DSSSDs
- ~35 % of 4π for βp/βα

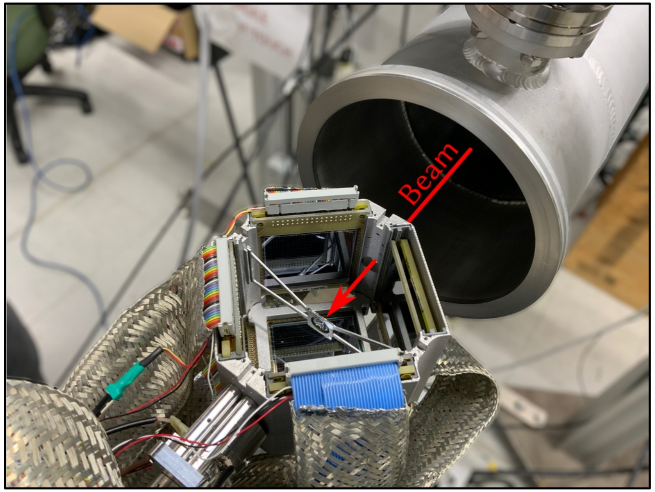

Silicon cube

- 6 ΔE–E silicon detector telescopes
- ΔE detectors are 16x16 DSSSDs
- ~35 % of 4π for βp/βα

Angular resolution ~4°, worst-case

- Good energy resolution from energy loss corrections

For β2p, detection efficiency depends on opening angle Θ_{2p} between 1st and 2nd proton

Simulations of various Θ_{2p} in setup geometry must correct for observed distributions of Θ_{2p}

Variation of Ω vs. Θ_{2p} reasonable; symmetric setup

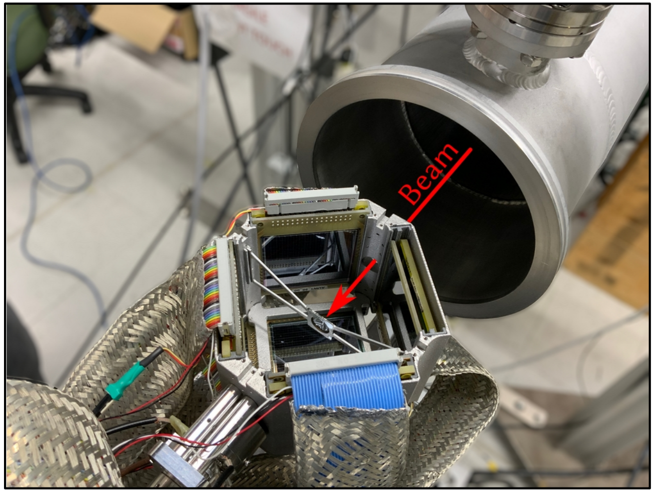

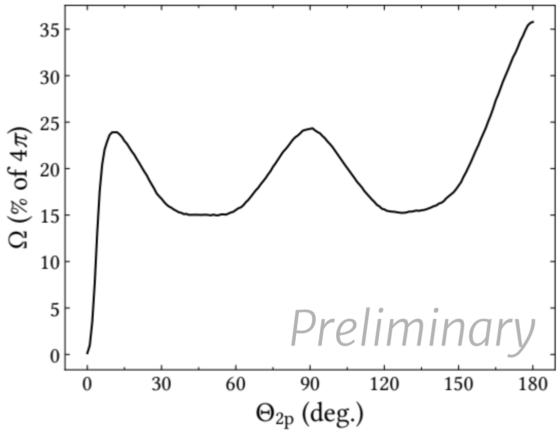

The data – ^{22}Al

Two-proton events:
Plot individual proton energies E_i against Q-value of two-proton decay Q_{2p}

Per Q_{2p} value there are two values of E_i

Previously, only two Q_{2p} peaks known:

- ^{22}Mg IAS → ^{21}Na* → ^{20}Ne 0+
- ^{22}Mg IAS → ^{21}Na* → ^{20}Ne 2+

Q_{2p} determined from E_1, E_2, Θ_{2p}:

$$Q_{2\mathrm{p}} = E_1 + E_2 + m_\mathrm{p}(E_1 + E_2 + 2\sqrt{E_1 E_2}\cos\Theta_{2\mathrm{p}})/M_{^{20}\mathrm{Ne}}$$

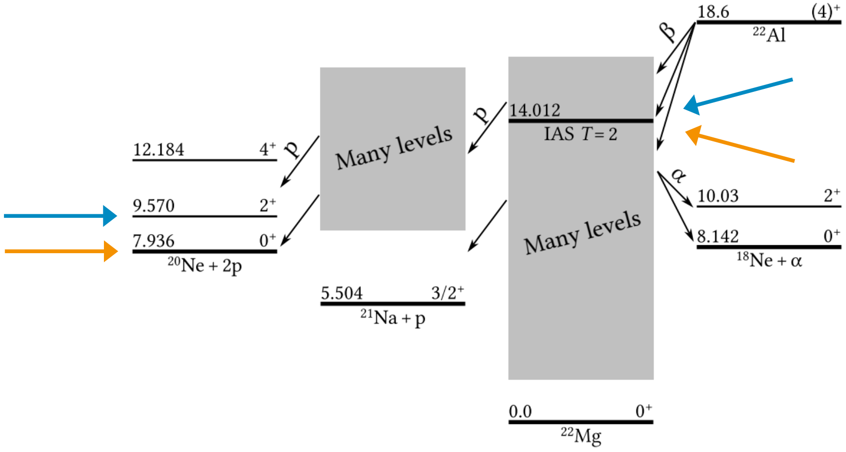

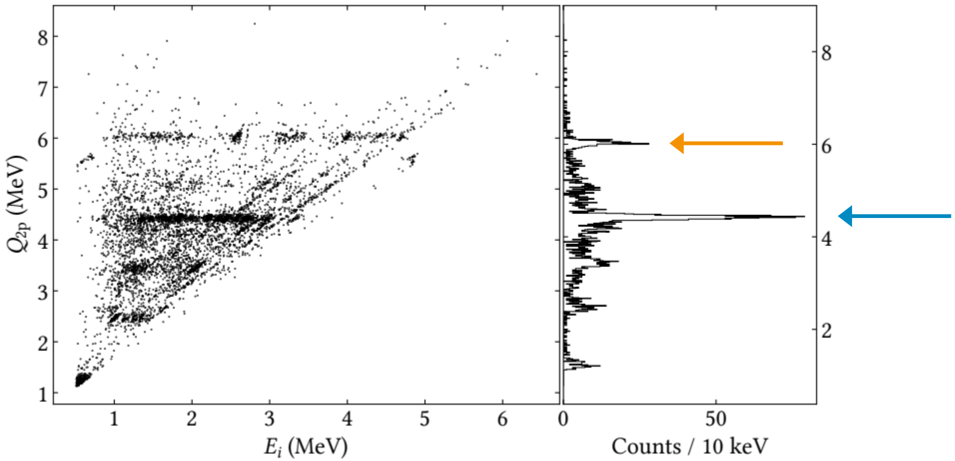

Sequential β2p

Q_{2p} determined from E_1, E_2, Θ_{2p}:

$$Q_{2p} = E_1 + E_2 + m_p(E_1 + E_2 + 2\sqrt{E_1 E_2}\cos\Theta_{2p})/M_{^{20}\mathrm{Ne}}$$

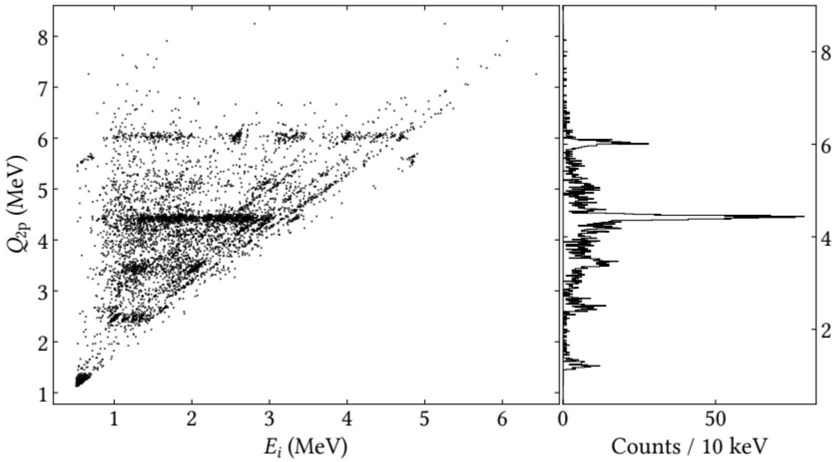

Sequential β2p

Understanding the „*Fynbo plot*“:

- For sequential decay, we have

$$\begin{aligned} Q_{2p} &= Q_1 + Q_2 \\ &= \frac{M_{^{21}\mathrm{Na}} + m_p}{M_{^{21}\mathrm{Na}}} E_1 + Q_2 \end{aligned}$$

  - i.e. 1st emitted proton generally follows straight line of slope ~1 with offset determined by energy release of 2nd proton, Q_2

Q_{2p} determined from E_1, E_2, Θ_{2p}:

$$Q_{2p} = E_1 + E_2 + m_p(E_1 + E_2 + 2\sqrt{E_1 E_2}\cos\Theta_{2p})/M_{^{20}\mathrm{Ne}}$$

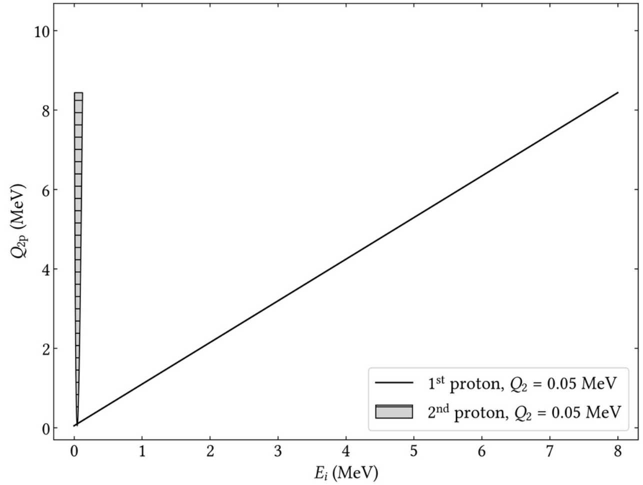

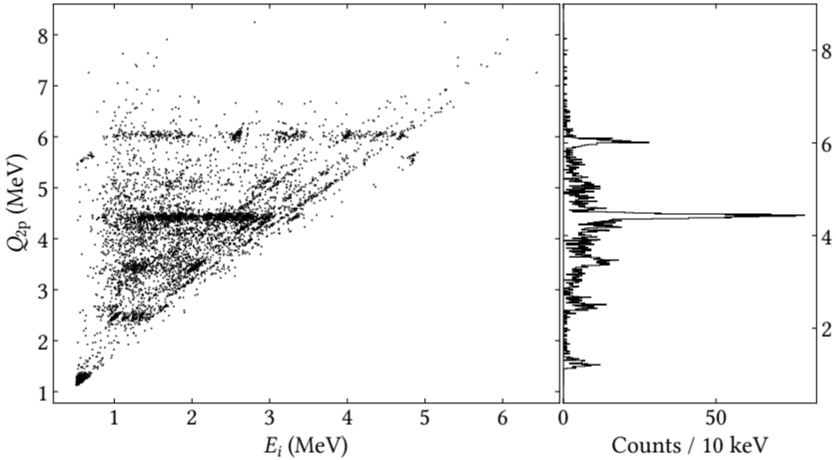

Sequential β2p

Understanding the „*Fynbo plot*“:

- For sequential decay, we have

$$\begin{aligned} Q_{2p} &= Q_1 + Q_2 \\ &= \frac{M_{^{21}\mathrm{Na}} + m_p}{M_{^{21}\mathrm{Na}}} E_1 + Q_2 \end{aligned}$$

  - i.e. 1st emitted proton generally follows straight line of slope ~1 with offset determined by energy release of 2nd proton, Q_2

Q_{2p} determined from E_1, E_2, Θ_{2p}:

$$Q_{2p} = E_1 + E_2 + m_p(E_1 + E_2 + 2\sqrt{E_1 E_2}\cos\Theta_{2p})/M_{^{20}\mathrm{Ne}}$$

Recoil broadening

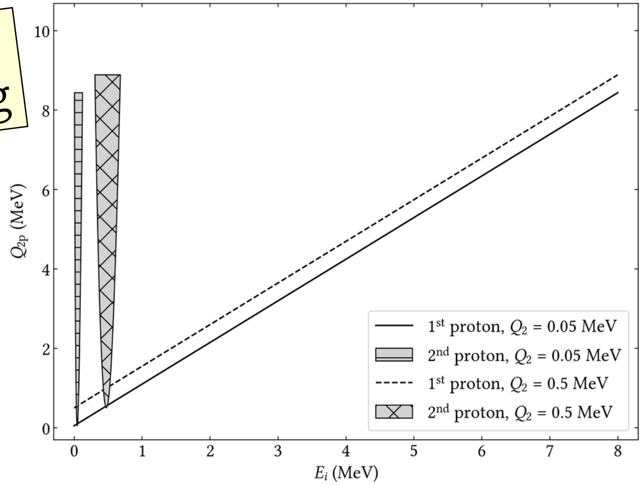

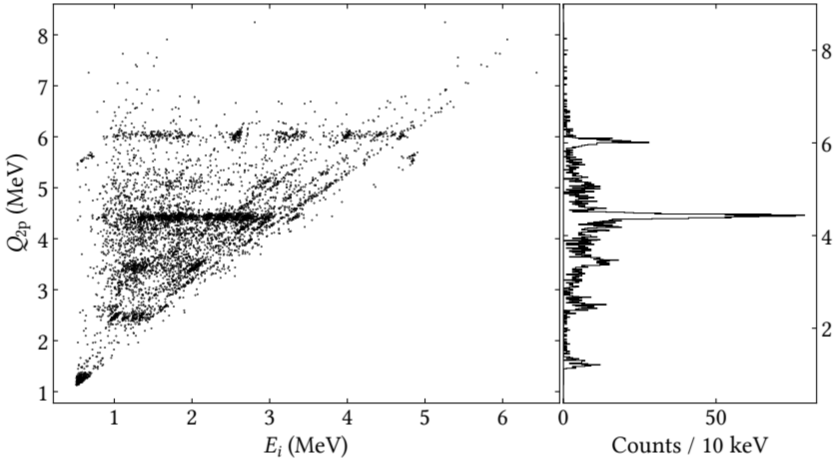

Sequential β2p

Understanding the „*Fynbo plot*“:

- For sequential decay, we have

$$\begin{aligned} Q_{2p} &= Q_1 + Q_2 \\ &= \frac{M_{^{21}\mathrm{Na}} + m_p}{M_{^{21}\mathrm{Na}}} E_1 + Q_2 \end{aligned}$$

  - i.e. 1st emitted proton generally follows straight line of slope ~1 with offset determined by energy release of 2nd proton, Q_2

Q_{2p} determined from E_1, E_2, Θ_{2p}:

$$Q_{2p} = E_1 + E_2 + m_p(E_1 + E_2 + 2\sqrt{E_1 E_2}\cos\Theta_{2p})/M_{^{20}\mathrm{Ne}}$$

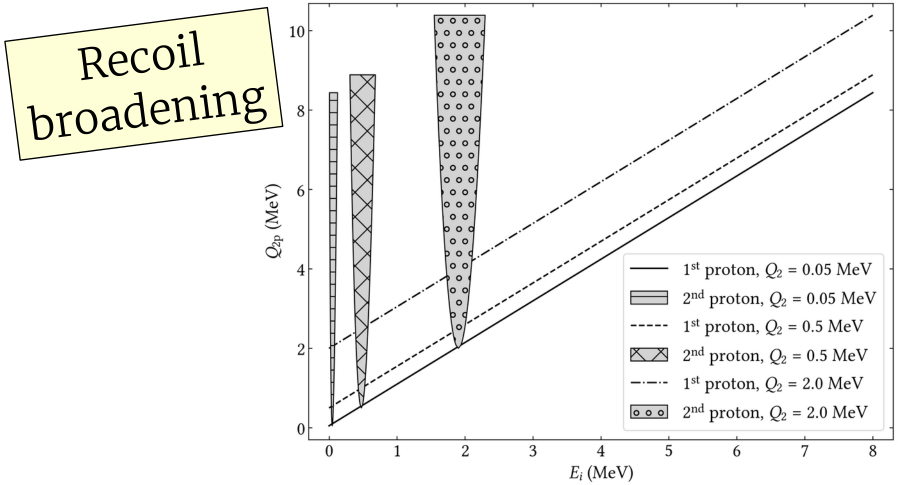

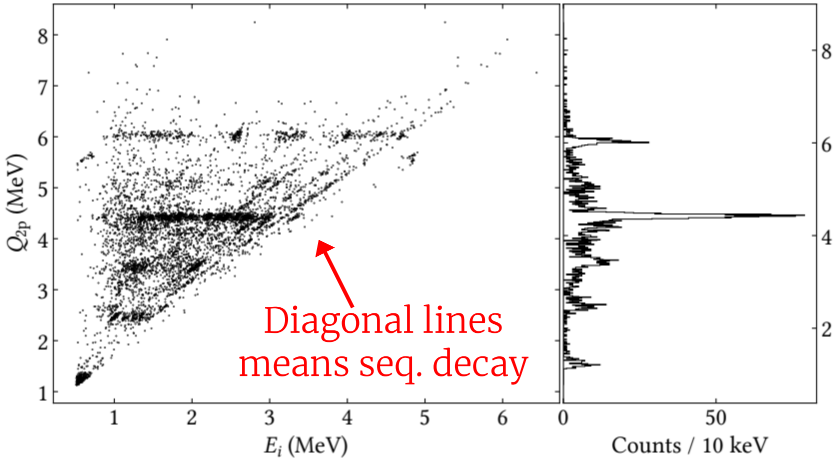

Sequential β2p

For sequential decay, we have:

$$\begin{aligned} Q_{2p} &= Q_1 + Q_2 \\ &= \frac{M_{^{21}\mathrm{Na}} + m_p}{M_{^{21}\mathrm{Na}}} E_1 + Q_2 \end{aligned}$$

Q_{2p} determined from E_1, E_2, Θ_{2p}:

$$Q_{2p} = E_1 + E_2 + m_p(E_1 + E_2 + 2\sqrt{E_1 E_2}\cos\Theta_{2p})/M_{^{20}\mathrm{Ne}}$$

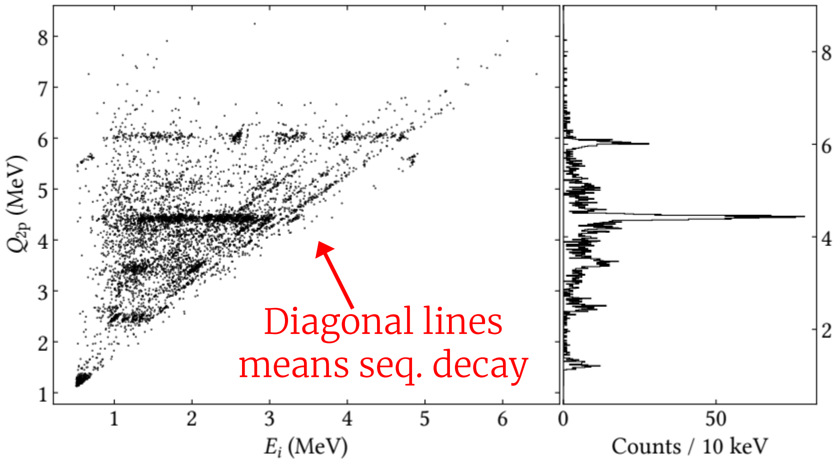

Sequential β2p

For sequential decay:
E_1 is constant w.r.t. $\cos\Theta_{2p}$, while
E_2 depends linearly on $\cos\Theta_{2p}$:

$$E_2 = E_2' + m_\mathrm{p}^2 E_1 / M_{^{21}\mathrm{Na}}^2 - 2m_\mathrm{p}\sqrt{E_1 E_2'}\cos\Theta_{2\mathrm{p}}/M_{^{21}\mathrm{Na}}$$

For sequential decay, we have:

$$\begin{aligned} Q_{2\mathrm{p}} &= Q_1 + Q_2 \\ &= \frac{M_{^{21}\mathrm{Na}} + m_\mathrm{p}}{M_{^{21}\mathrm{Na}}} E_1 + Q_2 \end{aligned}$$

Q_{2p} determined from E_1, E_2, Θ_{2p}:

$$Q_{2\mathrm{p}} = E_1 + E_2 + m_\mathrm{p}(E_1 + E_2 + 2\sqrt{E_1 E_2}\cos\Theta_{2\mathrm{p}})/M_{^{20}\mathrm{Ne}}$$

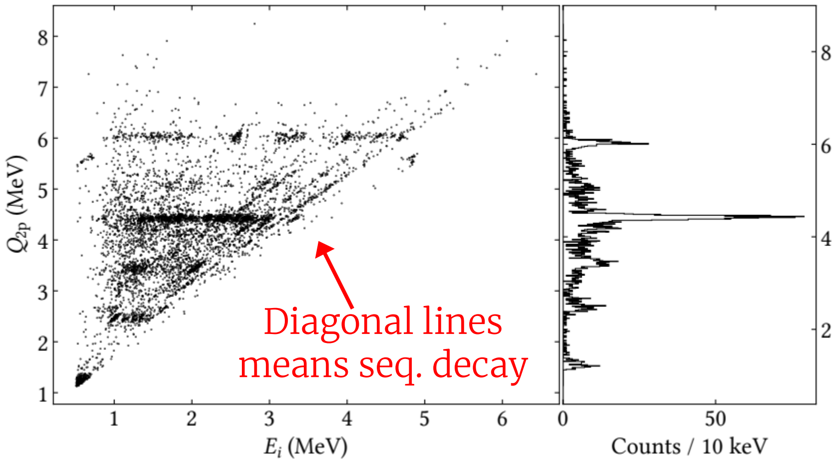

Sequential β2p

For sequential decay:
E_1 is constant w.r.t. $\cos\Theta_{2p}$, while
E_2 depends linearly on $\cos\Theta_{2p}$:

$$E_2 = E_2' + m_p^2 E_1 / M_{^{21}Na}^2 - 2m_p\sqrt{E_1 E_2'}\cos\Theta_{2p}/M_{^{21}Na}$$

Gating on specific Q_{2p} peaks allows us to examine population of intermediate states

For sequential decay, we have:

$$\begin{aligned} Q_{2p} &= Q_1 + Q_2 \\ &= \frac{M_{^{21}Na} + m_p}{M_{^{21}Na}} E_1 + Q_2 \end{aligned}$$

Q_{2p} determined from E_1, E_2, Θ_{2p}:

$$Q_{2p} = E_1 + E_2 + m_p(E_1 + E_2 + 2\sqrt{E_1 E_2}\cos\Theta_{2p})/M_{^{20}Ne}$$

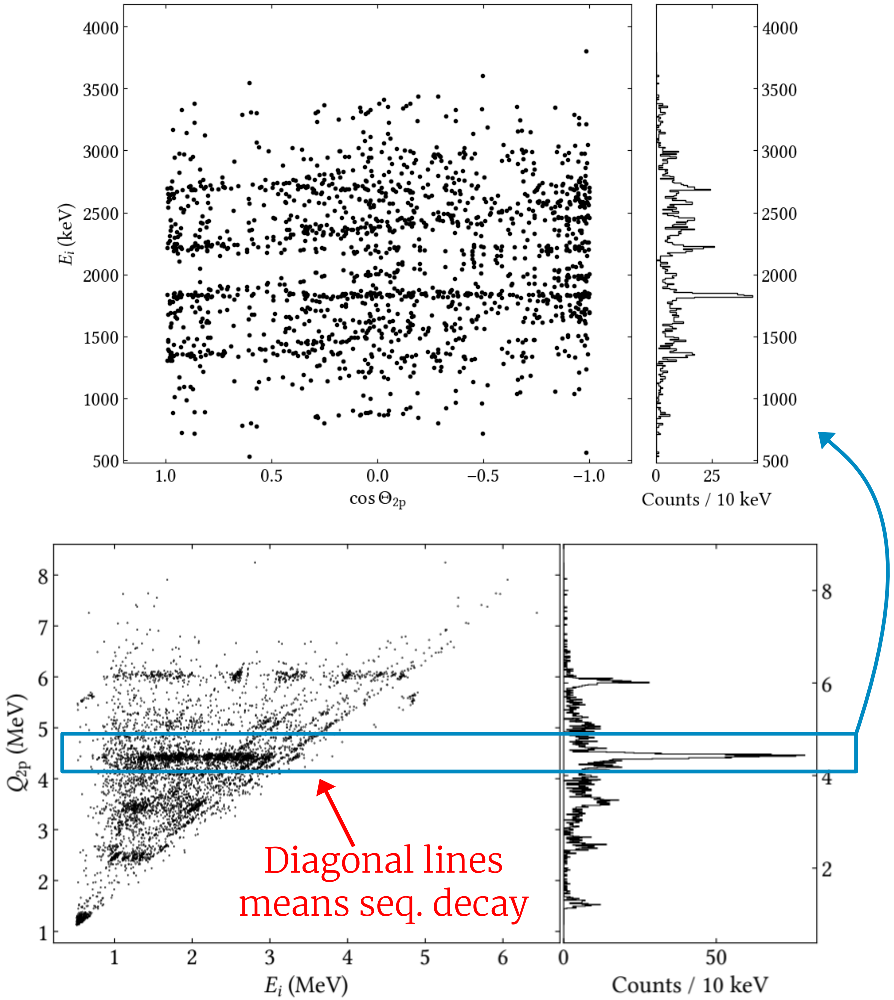

Sequential β2p

For sequential decay:
E_1 is constant w.r.t. $\cos\Theta_{2\mathrm{p}}$, while
E_2 depends linearly on $\cos\Theta_{2\mathrm{p}}$:

$$E_2 = E_2' + m_\mathrm{p}^2 E_1/M_{^{21}\mathrm{Na}}^2 - 2m_\mathrm{p}\sqrt{E_1 E_2'}\cos\Theta_{2\mathrm{p}}/M_{^{21}\mathrm{Na}}$$

Gating on specific $Q_{2\mathrm{p}}$ peaks allows us to examine population of intermediate states

For sequential decay, we have:

$$Q_{2\mathrm{p}} = Q_1 + Q_2 = \frac{M_{^{21}\mathrm{Na}} + m_\mathrm{p}}{M_{^{21}\mathrm{Na}}} E_1 + Q_2$$

$Q_{2\mathrm{p}}$ determined from E_1, E_2, $\Theta_{2\mathrm{p}}$:

$$Q_{2\mathrm{p}} = E_1 + E_2 + m_\mathrm{p}(E_1 + E_2 + 2\sqrt{E_1 E_2}\cos\Theta_{2\mathrm{p}})/M_{^{20}\mathrm{Ne}}$$

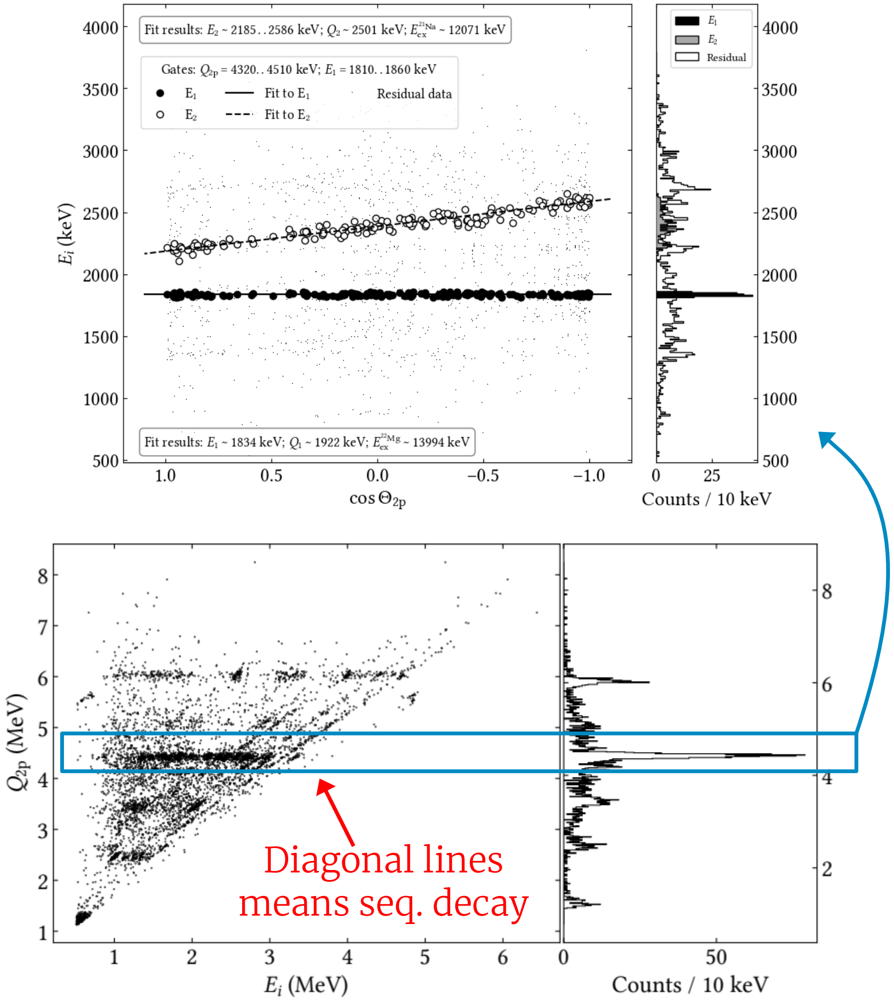

Sequential β2p

For sequential decay:
E_1 is constant w.r.t. $\cos\Theta_{2p}$, while
E_2 depends linearly on $\cos\Theta_{2p}$:

$$E_2 = E_2' + m_p^2 E_1 / M_{^{21}\mathrm{Na}}^2 - 2m_p \sqrt{E_1 E_2'} \cos\Theta_{2p} / M_{^{21}\mathrm{Na}}$$

Gating on specific Q_{2p} peaks allows us to examine population of intermediate states

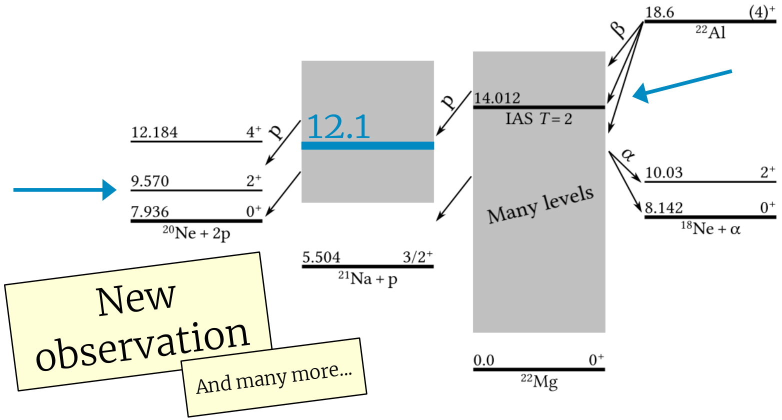

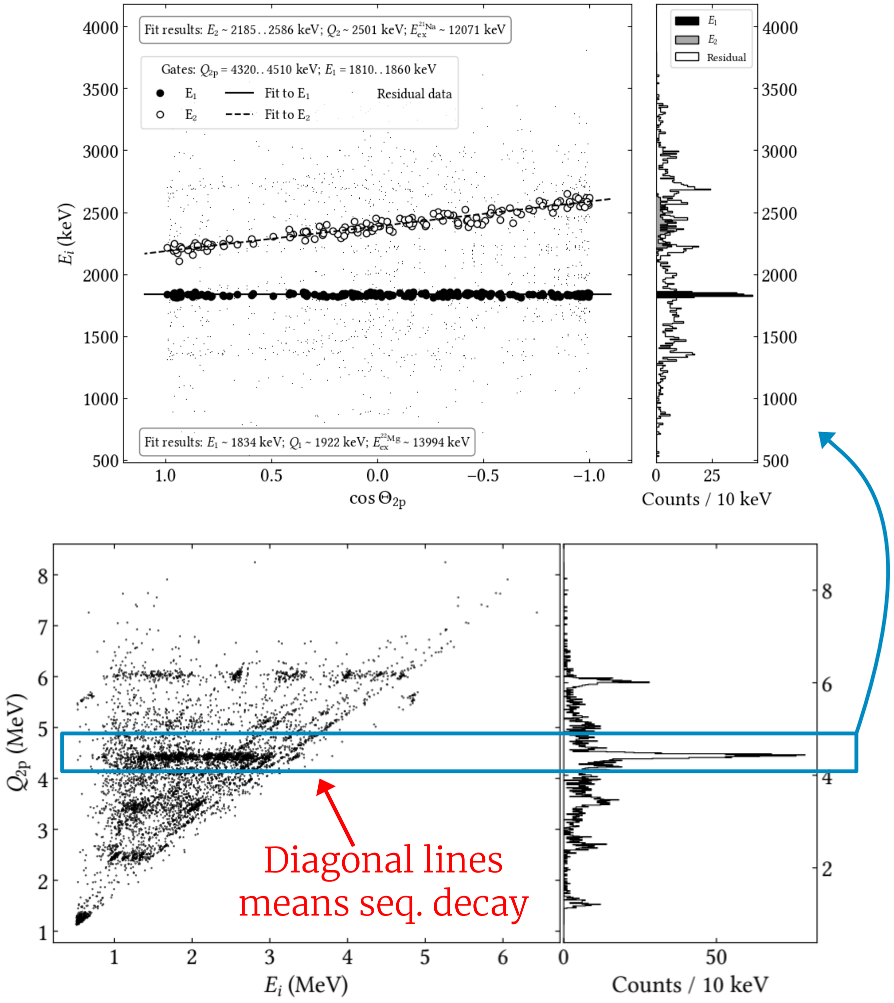

βα from ^{22}Al

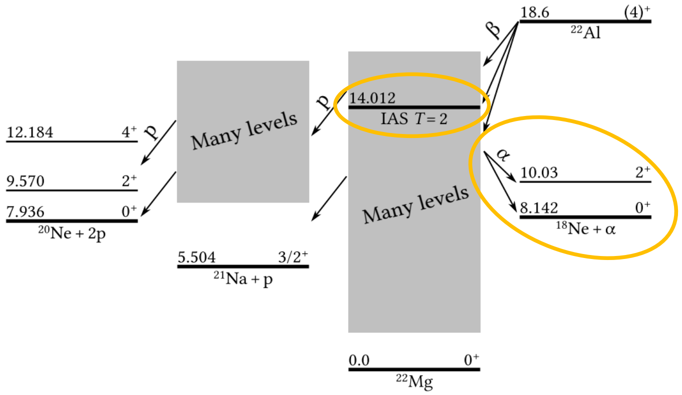

18.6
(4)+
22Al
β
14.012
IAS T = 2
p
Many levels
Many levels
p
12.184
4+
9.570
2+
7.936
0+
20Ne + 2p
5.504
3/2+
21Na + p
α
10.03
2+
8.142
0+
18Ne + α
0.0
0+
22Mg

βα from ^{22}Al

First observation of βα
from ^{22}Mg IAS to ^{18}Ne g.s.

This confirms J=4 assignment of IAS
and, hence, J=4 assignment of g.s. of ^{22}Al

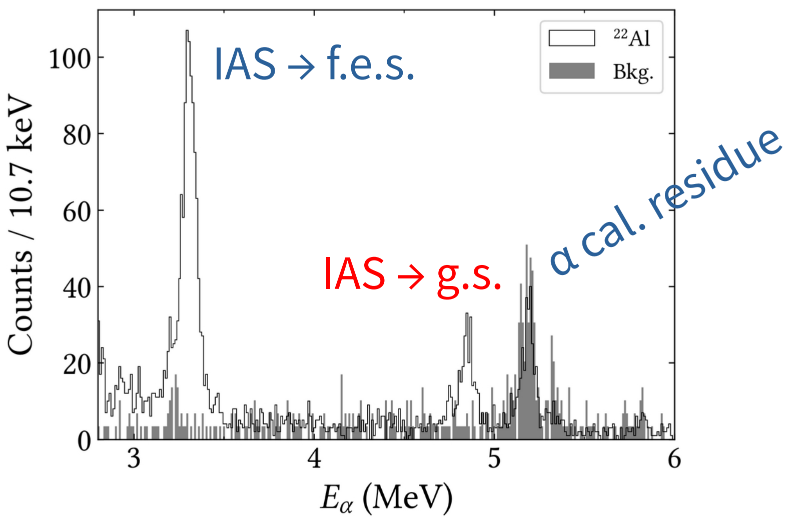

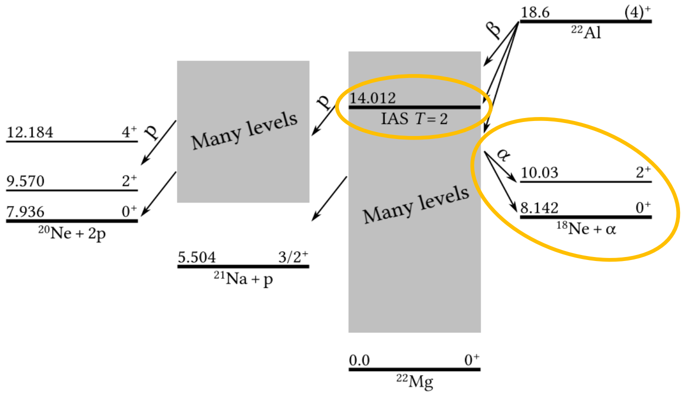

βα from ^{22}Al (and ^{26}P)

First observation of βα from ^{22}Mg IAS to ^{18}Ne g.s.

This confirms J=4 assignment of IAS and, hence, J=4 assignment of g.s. of ^{22}Al

Equivalent non-observation for ^{26}P suggests J=3

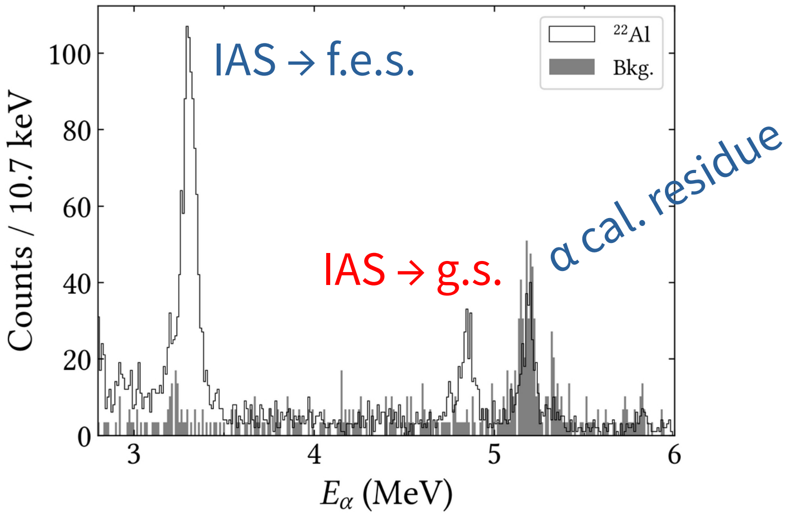

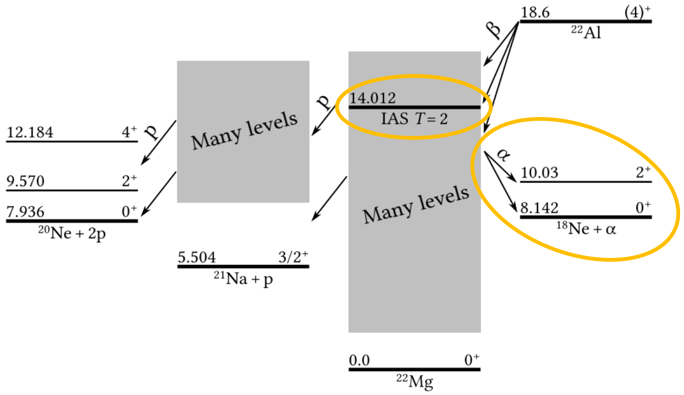

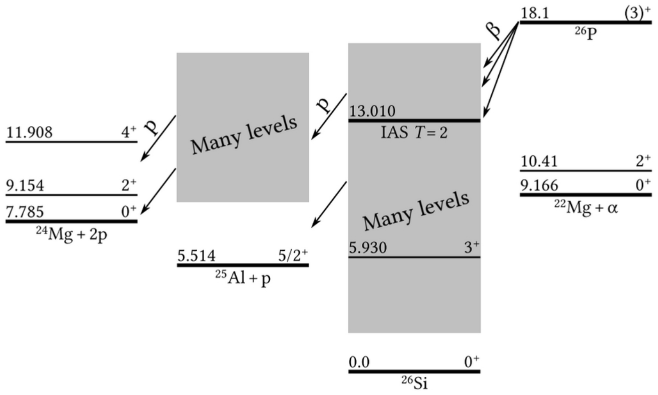

Summary and outlook

Takeaway:

- In-flight produdction rates and ISOL detection methods yield unprecedented results
- Many hitherto unobserved β2p channels
- βα discovery → nuclear structure

There is more:

- βp (conditioned on β2p)
- βpγ
- Sequential vs. direct β2p

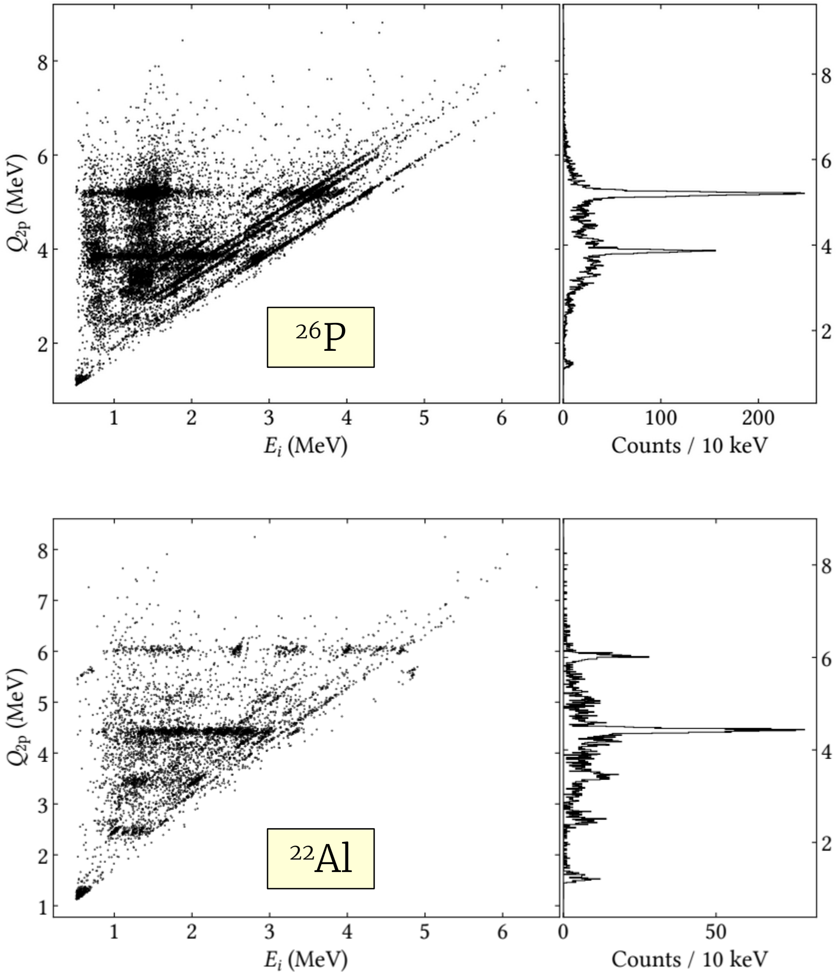

Thank you for your attention

Extra slides

Gas Stopper

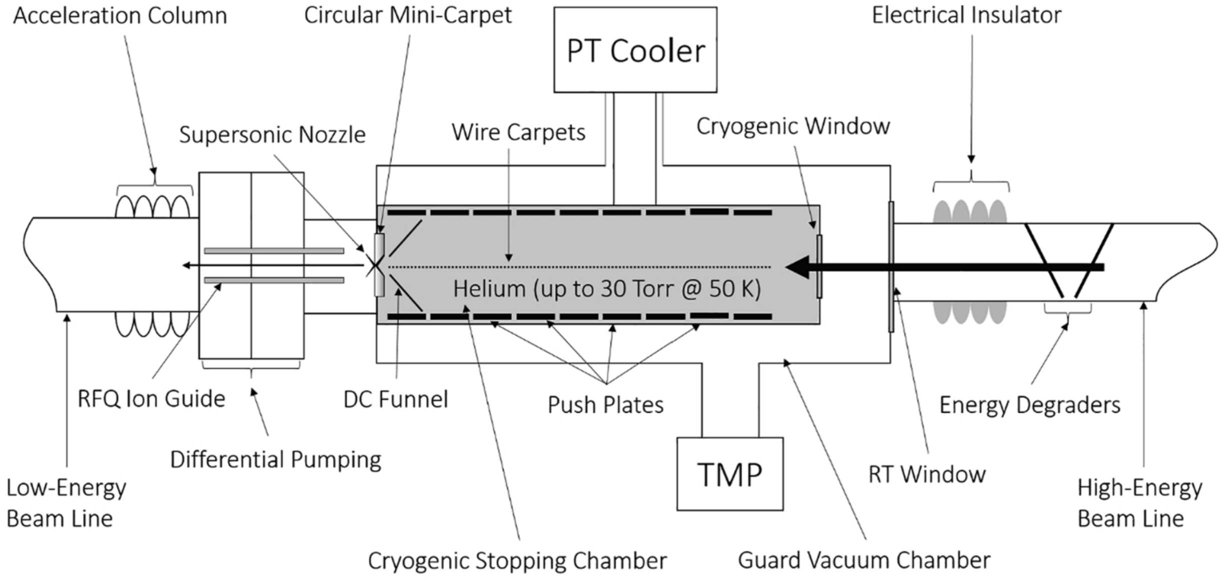

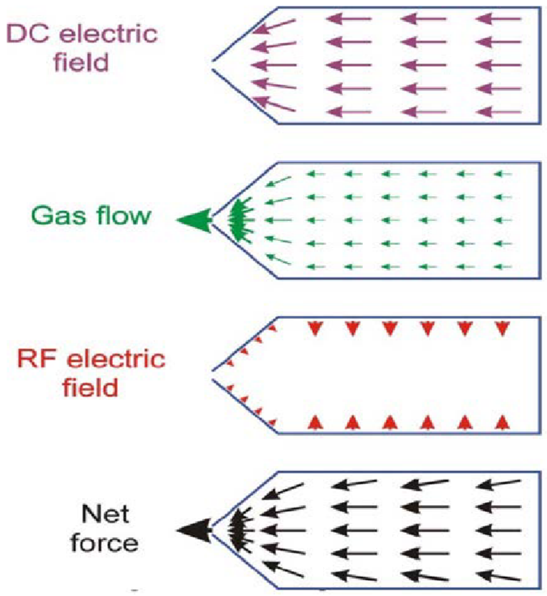

K.R. Lund, et al., Nuclear Inst. and Methods in Physics Research B 463 (2020) 378–381

Courtesy of Chandana Sumithrarachchi

Beta-delayed particle emission

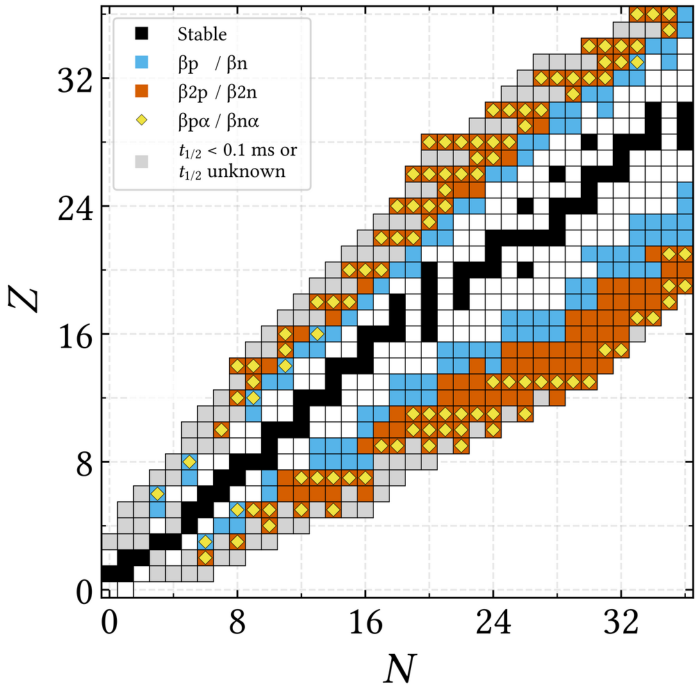

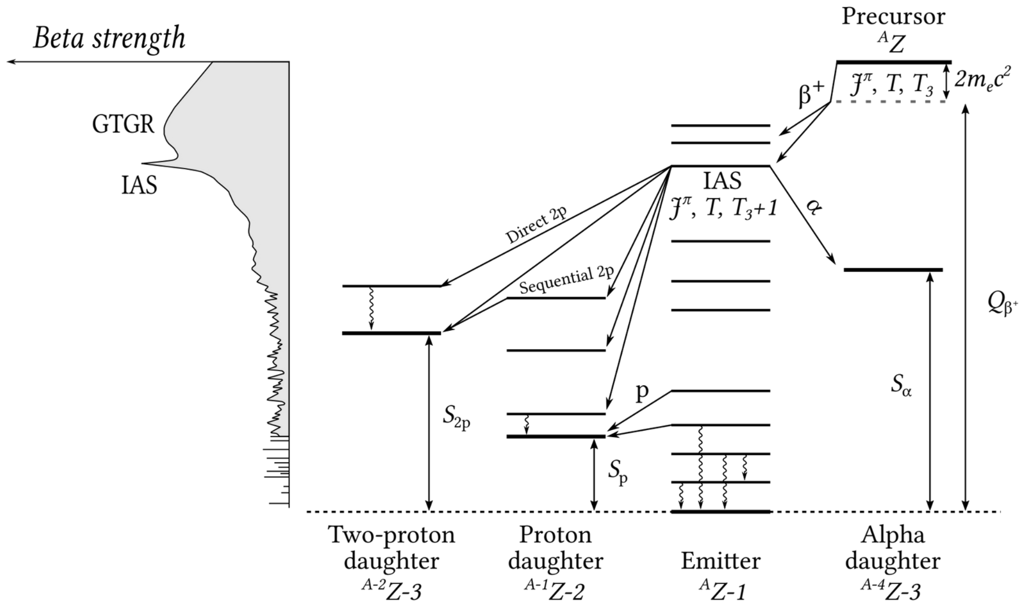

History

22Al first observed b2p emitter; 26P second

2.5.2. First observation of $\beta 2p$ decay and later experimental results

It was indeed beneath the odd–odd $T_z = -2$ nuclei that the first $\beta 2p$ emitters were observed. After its identification by βp emission, ^{22}Al was discovered to decay via this new nuclear decay mode [220]. The nuclei of interest were produced by a ^{3}He induced reaction on a ^{24}Mg target.

(...)

The second $\beta 2p$ emitter was identified by the same group a few months later [223]. It was again a light odd–odd $T_z = -2$ nucleus, ^{26}P, as predicted by Goldanskii [218]. Contrary to ^{22}Al, where different 2p emission paths could be identified, ^{26}P seems to decay by only one 2p path. This difference is most likely due to the different nuclear structure of the one-proton daughter nuclei, ^{21}Na and ^{25}Al.

B. Blank, M.J.G. Borge, Progress in Particle and Nuclear Physics 60 (2008) 403–483

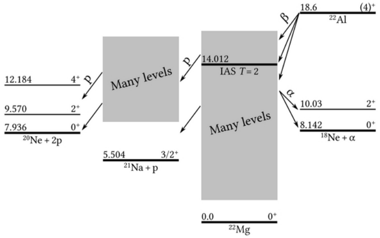

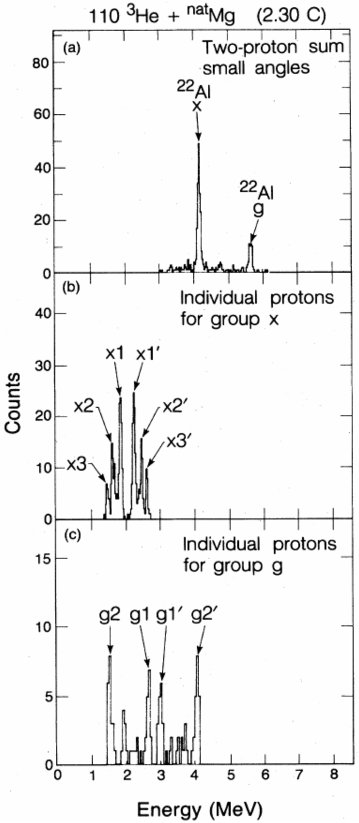

M.D. Cable, et al., Phys. Rev. C 30 (1984) 1276

New data

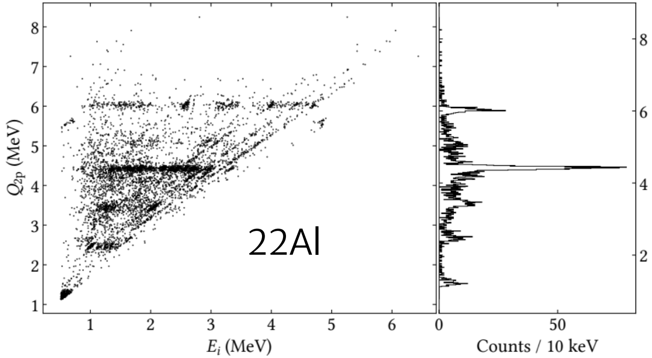

New data